ANAMET REPORT

ANAMET Report 052
August 2010

ANAMET 052: Comparison of Type-N sliding loads from 2 to 18 GHz

M J Salter

NPL National Physical Laboratory

The National Physical Laboratory is operated on behalf of the DTI by NPL Management Limited, a wholly owned subsidiary of Serco Group plc

This report has been approved by the ANAMET Steering Committee.

Further information about ANAMET can be found at: www.npl.co.uk/anamet

Comments on this report should be sent to: anamet@npl.co.uk

ANAMET 052: Comparison of Type-N sliding loads from 2 to 18 GHz

Martin J Salter
National Physical Laboratory, Teddington, UK
August 2010

1 Introduction

The purpose of this report is to present the results of the round robin measurement comparison exercise designated 'ANAMET 052' that was run by ANAMET between December 2005 and June 2007.

During this exercise, ten participating organizations measured the voltage reflection coefficients (VRCs) of a pair of coaxial sliding loads fitted with precision Type-N connectors (one male and one female) at 65 frequencies between 2 GHz and 18 GHz for different slider positions. Based on these VRC measurements, each participant estimated the centres and radii of the circles defined by the sliding loads in the VRC plane as a function of frequency allowing a comparison to be made of the estimates of the different participants.

The plan of the report is as follows. Basic details of the measurement comparison (the devices, the measurands, the participants and the timescale) are given in Section 2. The VRC measurement methods and circle fitting algorithms used by the participants are tabulated in Section 3. Section 4 describes the method used to provide a statistical analysis of the results. The results are summarised in Section 5. A discussion is provided in Section 6 and conclusions are stated in Section 7.

1.1 Sliding terminations

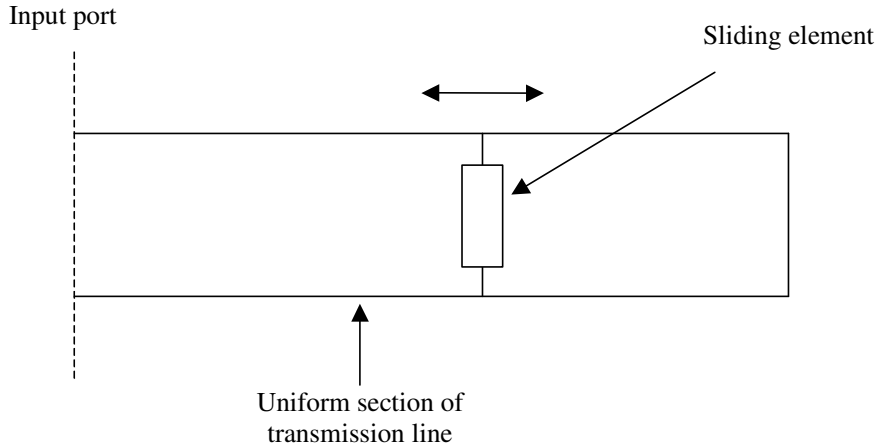

Figure 1: Schematic diagram of a sliding termination

Sliding loads (i.e. low reflection sliding terminations) as well as sliding short-circuits (i.e. high reflection sliding terminations) are widely used in microwave measurements. They consist of a sliding element which is free to slide along a

uniform section of transmission line as shown schematically in Figure 1. The transmission line can be either coaxial line or rectangular waveguide.

Ideally the transmission line section should have no loss and characteristic impedance equal to the required system impedance and be fitted with a precision coaxial connector or waveguide flange to minimise any reflection arising at the input. Neglecting any loss in the transmission line section and any reflection arising at its input, the reflection coefficient of the sliding termination is given by

$$\Gamma = r\exp\left[j(\Theta_0 - 2\beta l)\right]$$

where r and Θ_0 are, respectively, the magnitude and phase of the reflection coefficient of the sliding element, β is the phase constant of the transmission line section and l is the distance of the sliding element from the input of the transmission line section.

As the position of the sliding element is varied in the transmission line section, the input reflection coefficient of the sliding termination traces out a circle in the reflection coefficient plane. The centre of the circle is related to the reflection arising at the input to the transmission line section [in practice the centre of the circle is not exactly at the origin of the complex VRC plane as implied by the above equation] and the radius of the circle is related to the magnitude of the reflection arising at the sliding element. A sliding termination is usually measured with the sliding element set to a number of positions and a circle is fitted to the resulting reflection coefficient points at each frequency. When observed through a 2-port network (such as an adapter or a Automatic Network Analyser (ANA) error box), the transformed reflection coefficient again traces out a circle. This is because the transformation of reflection coefficient through a 2-port network takes the form of a bilinear transformation which maps circles to circles [1].

Applications of sliding terminations include the calibration of ANAs and the measurement of adapter efficiency [2, 3]. Kasa [4] describes two 1-port ANA calibration methods involving (i) one sliding termination and two known loads and (ii) two sliding terminations (one low reflection and one high reflection) and one known load. In Kasa's analysis, r, Θ_0, β and l do not need to be known; all that is required is that r and Θ_0 are constant. Engen [5] extended Kasa's work by accounting for the effect of loss in the transmission line section of the sliding terminations.

2 Details of the ANAMET-052 comparison

2.1 Devices

Figure 2: The male and female Type-N sliding loads circulated during the comparison

The devices that were circulated amongst the participants during the comparison are shown in Figure 2. They comprise a Maury Microwave Corporation 8834C Type-N sliding load kit consisting of a Model 8834A Type-N female termination (s/n 4061) and a Model 8834B Type-N male termination (s/n 4104). The Type-N connectors in the two terminations are unsupported (i.e. beadless) and the female connector is a precision slotless connector. The devices were supplied in a foam lined wooden carrying case that was used to house the devices during shipment between the participants.

2.2 Measurands

The measurands (measured from 2 to 18 GHz in 0.25 GHz steps i.e. at a total of 65 frequencies) were as follows for both the male and the female sliding loads:

1. The centre of the circle defined by the sliding load in the complex VRC plane;
2. The radius of the circle defined by the sliding load in the complex VRC plane;
3. The complex-valued Voltage Reflection Coefficient (VRC) of the sliding load with the sliding element set to four specified positions.

The four sliding element positions for measurand (3) were as follows: the sliding element set to the two end stops and to two marked notch positions on each sliding load.

The centre and radius of the circle (measurands (1) and (2)) are determined by measuring the VRC of the sliding load for a number of sliding element positions and fitting a circle to the resulting data at each frequency. The choice of sliding element positions to be used to determine the circle parameters was left up to the participants. The positions specified for measurand (3) were not intended to restrict this choice.

In addition to the above measurands, the participants were also asked to supply the following additional data:

4. Any complex-valued VRC values used to determine the circle parameters in addition to those specified in (3)[1];
5. The connector pin-depths (in inches or millimetres) for each of the two sliding loads.

The participants were asked to avoid adjustment of the positions of the sliding load centre conductors as much as possible and to report any such necessary adjustments to the co-ordinator of the comparison.

In this report, attention is focussed on the circle parameters i.e. on presenting and analysing the values obtained by the participants for measurands (1) and (2).

2.3 Participants

The participating organizations and the contacts from each organization are listed in Table 1. The anonymity of the participants' results has been preserved by using labels (i.e. A, B, etc), which have been applied arbitrarily.

Table 1: Participants in the ANAMET 052 measurement comparison

Company/ organisation	**Location**	**Contact**
Aeroflex	Stevenage, UK	Steve Worrall Doug Skinner
ASAP	Farnborough, UK	Steve Harter Pete Constable
CMI	Czech Republic	Karel Drazil
INTA	Spain	Manuel Rodriguez
METAS	Switzerland	Juerg Ruefenacht
NMI	Netherlands	Jan de Vreede
NMIJ, AIST	Japan	Masahiro Horibe
NPL	Teddington, UK	Martin Salter
Saab Metech AB	Sweden	Patrik Persson Mikael Rydstedt
TUBITAK-UME	Turkey	Senel Yaran

2.4 Timescale

Measurements on the devices were carried out by the participants between December 2005 and June 2007.

[1] All the participants made use of the VRC measurements in measurand (3) in the determination of the circle parameters. Some also chose to make extra VRC measurements in addition to those in measurand (3) to determine the circle parameters.

The female sliding load was damaged in March 2006 and was subsequently repaired. Three participants measured the device before it was damaged and eight measured it after it was repaired as shown in Table 2. Note that one participant (participant A) measured the device twice: once before damage (A1) and once after repair (A2). Because the characteristics of the device changed as a result of the damage and repair, the two sets of measurements identified in Table 2 are treated separately in the analysis of the results of the comparison.

Table 2: Measurements on the female sliding load before and after it was damaged

Participants measuring female sliding load **before** damage (3 participants)	A1, B, C
Participants measuring female sliding load **after** repair (8 participants)	D, A2, E, F, G, H, I, J

3 Measurement methods & circle fitting algorithms used during the comparison

The VRC measurement methods and circle fitting methods used by the participants are summarised in Tables 3 and 4 based on information supplied by the participants. The VRC measurement method is described by the type of Automatic Network Analyser (ANA) and the ANA calibration method used. The circle fitting method is described by the number of slider positions used to determine the circle and the circle fitting algorithm used. The circle fitting algorithms are briefly described in Section 3.1.

Table 3: VRC measurement methods used by the participants

ANA used to measure VRC	
8510C	A, C, D, E, F, H, I, J
PNA	G
8722C	B
ANA calibration method	
S-O-L/SL-T[2]	B, C[3], D[4], E, F, H, I, J
LRL[5]	A
Multiline TRL[6]	G

[2] S-O-L/SL-T = Short-Open-Load/ Sliding Load-Thru.
[3] Additional corrections made for residual directivity.
[4] Sliding load and broadband load.
[5] LRL = Line-Reflect-Line.
[6] Multiline TRL = a version of Thru-Reflect-Line (TRL) in which more than one line is used at a given frequency thereby over determining the calibration.

Table 4: Circle fitting methods used by the participants

Number of slider positions used to fit circle	
20	F
9	J
7	A, C
6	D, E
5	B
4	G, H, I
Circle fitting algorithm	
Method 1 (Kasa's method/ Linear least squares method)	A, B, D, E, F, G, H, I, J
Method 2 (Mean radius method)	C

3.1 Circle fitting algorithms used by the participants

Two different least squares methods were used by the participants to fit circles to measured VRC values each involving a different sum of squares objective function to be minimised. The details of the numerical methods used to perform the minimisation were not specified by the participants. Suitable numerical methods are described in [6]. In the description of the methods, it is assumed that there are N ($N \geq 3$) data points (x_1, y_1), (x_2, y_2), …, (x_N, y_N) to which a circle is to be fitted. The circle centre is denoted (A, B) and the circle radius is denoted R. Method 1 results in a linear least squares problems whilst method 2 results in a non-linear least squares problem.

3.1.1 Method 1 (Kasa's method/ Linear least squares method)

The objective function to be minimised is [7]:

$$\sum_{i=1}^{N}\left[r_i^2 - R^2\right]^2$$

where $r_i = \sqrt{(x_i - A)^2 + (y_i - B)^2}$ is the distance of the ith point (x_i, y_i) from the circle centre (A, B) and R is the circle radius. The objective function can be written

$$u(A,B,C) = \sum_{i=1}^{N}\left[\left(x_i^2 + y_i^2\right) - 2x_iA - 2y_iB + C\right]^2$$

where $C = A^2 + B^2 - R^2$. Minimising u with respect to A, B and C is a linear least squares problem. The circle centre is taken to be (A, B) and the circle radius is taken to be $R = \sqrt{A^2 + B^2 - C}$.

The objective function arises when solving the conditions for the N points to lie on a circle (namely $r_i^2 = R^2$, $i = 1, ..., N$) for A, B and C in a least squares sense.

A, B and C can be obtained by solving the normal equations for the problem which are

$$DQ = E$$

where (with all sums ranging from $i = 1$ to $i = \mathrm{N}$)

$$D = \begin{pmatrix} 2\sum x_i & 2\sum y_i & N \\ 2\sum x_i^2 & 2\sum x_i y_i & \sum x_i \\ 2\sum x_i y_i & 2\sum y_i^2 & \sum y_i \end{pmatrix}$$

$$Q = \begin{pmatrix} A \\ B \\ C \end{pmatrix}$$

$$E = \begin{pmatrix} \sum \left(x_i^2 + y_i^2\right) \\ \sum \left(x_i^3 + x_i y_i^2\right) \\ \sum \left(x_i^2 y_i + y_i^3\right) \end{pmatrix}.$$

The normal equations are obtained by setting the partial derivatives of u with respect to A, B and C equal to zero. Forming and solving the normal equations is not necessarily the best method to obtain the least squares solutions [6].

3.1.2 Method 2 (Mean radius method)

The objective function to be minimised is:

$$\sum_{i=1}^{N} \left[r_i - \bar{r}\right]^2$$

where $r_i = \sqrt{(x_i - A)^2 + (y_i - B)^2}$ is the distance of the ith point (x_i, y_i) from the circle centre (A, B) and $\bar{r}$ is the mean distance from the centre

$$\bar{r} = \frac{1}{N}\sum_{j=1}^{N} r_j = \frac{1}{N}\sum_{j=1}^{N} \sqrt{(x_j - A)^2 + (y_j - B)^2}\ .$$

The objective function can be written

$$w(A,B) = \sum_{i=1}^{N} \left[\sqrt{(x_i - A)^2 + (y_i - B)^2} - \frac{1}{N}\sum_{j=1}^{N} \sqrt{(x_j - A)^2 + (y_j - B)^2} \right]^2 .$$

Minimising w with respect to A and B is a non-linear least squares problem which is solved using an iterative method. The mean x and y coordinates of the points are taken as initial estimates for A and B. The circle centre is taken to be (A, B) and the circle radius is taken to be the mean distance of the points from the centre, $\bar{r}$.

4 Statistical analysis of the results

Because of the change in the characteristics of the female sliding load after it was damaged and subsequently repaired, the following data sets are analysed separately:

- Data for the male sliding load (10 estimates for each measurand);
- Data for the female sliding load before damage (3 estimates for each measurand – see Table 2);
- Data for the female sliding load after repair (8 estimates for each measurand - see Table 2).

4.1 Summary statistics for the participants' measurements

For the circle centres and circle radii, the collection of participants' measurements at each frequency are summarised by a consensus value and a measure of the dispersion about that value.

For the circle centres, the consensus value is calculated as the spatial median of the participants' values (i.e. as a point in the plane) and the measure of dispersion is calculated as the median absolute deviation (MAD) of the values from the spatial median (i.e. as a real number).

The spatial median is defined as the point in the plane which minimises the sum of the distances from the point to the participant's values. In other words, for participants' values $\{(x_i, y_i) : i = 1, 2, \ldots, n\}$, the expression

$$\sum_{i=1}^{N} \sqrt{(x_i - \mu_x)^2 + (y_i - \mu_y)^2}$$

is a minimum (over all possible choices of the point $\mu = (\mu_x, \mu_y)$) when μ is the spatial median.

The median absolute deviation (MAD) is defined as the median of the distances of the participants' values from the spatial median

$$MAD = median\left\{\sqrt{(x_i - \mu_x)^2 + (y_i - \mu_y)^2} : i = 1, 2, \ldots, n\right\}$$

The spatial median and the MAD define the centre and radius of a circle in the plane (the "MAD circle") that contains half of the participants' values.

For the circle radii, the consensus value is calculated as the median of the participants' values and the measure of dispersion is calculated as the median absolute deviation (MAD) of the participants' values from the median. The median and MAD define the mid point and half-length of an interval on the line (the "MAD interval") that contains half of the participants' values.

The summary statistics used to specify a consensus value and a measure of dispersion for the circle centres and the circle radii are listed in Table 5. These statistics are

"robust" in the sense that they are relatively unaffected by the presence of outliers in the data [8].

Table 5: The measurands and the statistics used to summarise them in the statistical analysis of the comparison

Measurand	Dimensionality of measurand[7]	Summary statistics	
		Consensus value	Measure of dispersion
Centre of circle	2D	Spatial median	MAD (i.e. median distance of values from spatial median)
Radius of circle	1D	Median	MAD (i.e. median distance of values from median)

4.2 Detecting values close to and far from the consensus value amongst the participants' measurements

The performance of a participant in measuring a particular measurand in the comparison is summarised by:

1. The percentage of frequencies at which the participant's values are close to the consensus value, and
2. The percentage of frequencies at which the participant's values are far from the consensus value (such values are called "unusual" or "outlying").

These percentages are obtained by calculating the Z-score, z, for each measured value defined as

$$z = \frac{AD}{MAD},$$

where AD (absolute deviation) is the distance of the value from the consensus and MAD (median absolute deviation) is the median distance from the consensus for all the values.

The measured value is considered to be:

- Close to the consensus value if it is in the MAD circle or MAD interval i.e. if $z<1$;
- Far from the consensus value i.e. unusual if $z>3$ for a circle radius [a one dimensional measurand] or if $z>3.75$ for a circle centre [a two dimensional measurand][8].

[7] 2D = two dimensional, 1D = one dimensional.

[8] The choice of threshold values for z used to identify "unusual" values is somewhat arbitrary. The threshold values of 3 and 3.75 for one dimensional and two dimensional data, respectively, arise as 1.5×2 and 1.5×2.5 where 1.5 is the approximate factor which multiplies MAD to give standard deviation for a normal distribution and 2 and 2.5 are coverage factors for 95% coverage probability in one dimension and two dimensions respectively.

4.3 Overall variability of the participants' measurements

For a particular measurand at a given frequency, the MAD gives a measure of the variability of the measurand between the participants at that frequency. The maximum MAD achieved provides a concise one figure summary of the variability of the measurand across the entire frequency range 2-18 GHz.

5 Results

Circle centre and circle radius results from the comparison are presented in Figures 3-14. The percentage of frequencies at which each participant's values are either close to or far from the consensus value are indicated in Tables 8-13. Finally, Table 14 gives an overall measure of variability for each of the measurands for each of the devices. The Figures and Tables used to present the results are listed in Tables 6 and 7.

Table 6: Figures used to present the results

Figure	Parameter	Device
3	Linear magnitude of circle centre	Male sliding load
4	Distances of measured circle centres from consensus value	Male sliding load
5	Circle radius	Male sliding load
6	Distances of measured circle radii from consensus value	Male sliding load
7	Linear magnitude of circle centre	Female sliding load (before damage)
8	Distances of measured circle centres from consensus value	Female sliding load (before damage)
9	Circle radius	Female sliding load (before damage)
10	Distances of measured circle radii from consensus value	Female sliding load (before damage)
11	Linear magnitude of circle centre	Female sliding load (after repair)
12	Distances of measured circle centres from consensus value	Female sliding load (after repair)
13	Circle radius	Female sliding load (after repair)
14	Distances of measured circle radii from consensus value	Female sliding load (after repair)

Table 7: Tables used to present the results

Table	Parameter	Device
8	Percentage of values close to consensus	Male sliding load
9	Percentage of values which are unusual	Male sliding load
10	Percentage of values close to consensus	Female sliding load (before damage)
11	Percentage of values which are unusual	Female sliding load (before damage)
12	Percentage of values close to consensus	Female sliding load (after repair)
13	Percentage of values which are unusual	Female sliding load (after repair)
14	Overall variability of the measurands	All

5.1 Results for the Male Sliding load

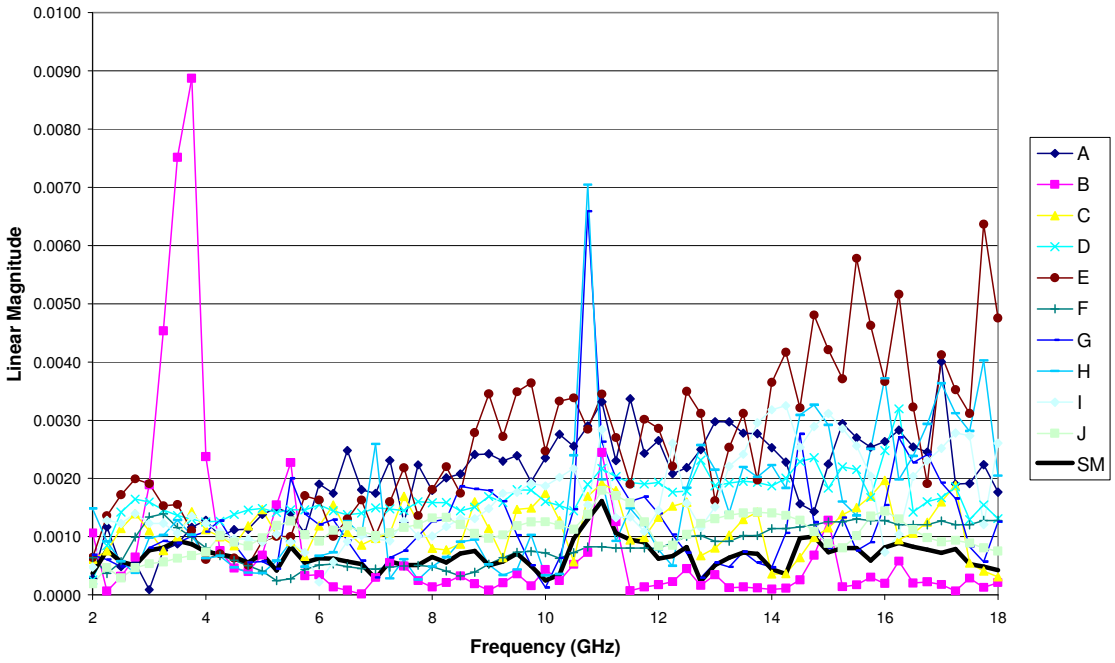

Figure 3: Linear magnitude of the circle centre for the male sliding load. The linear magnitude of the spatial median (SM) of the circle centres is also shown.

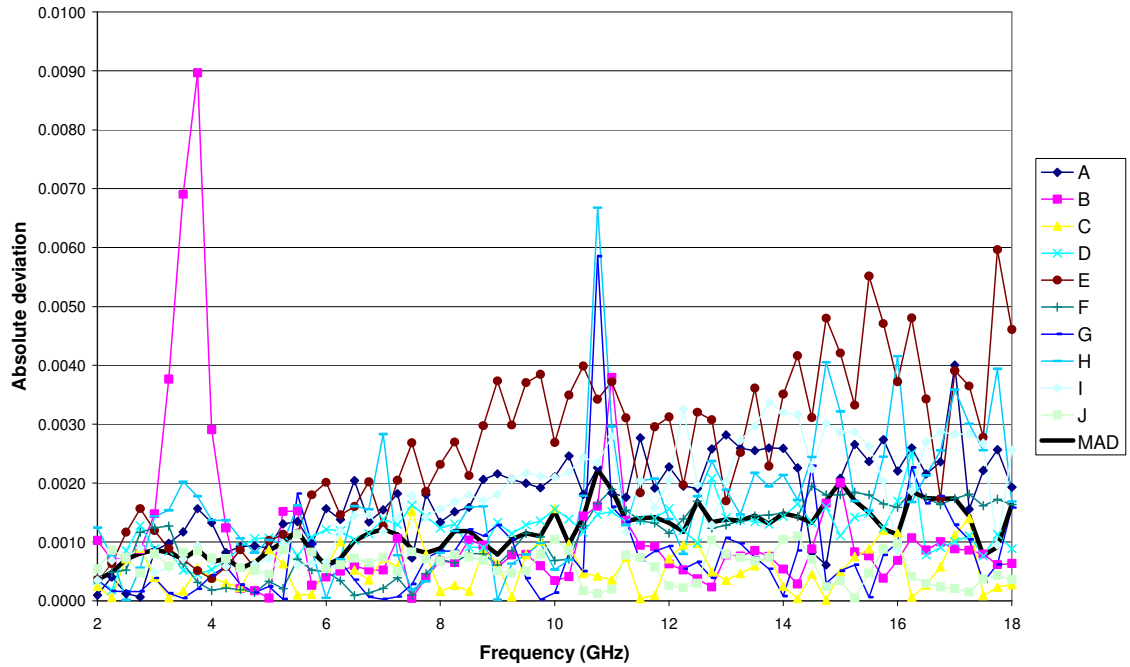

Figure 4: Absolute deviations of the measured circle centres from the spatial median of the circle centres for the male sliding load. Also shown is the median absolute deviation (MAD).

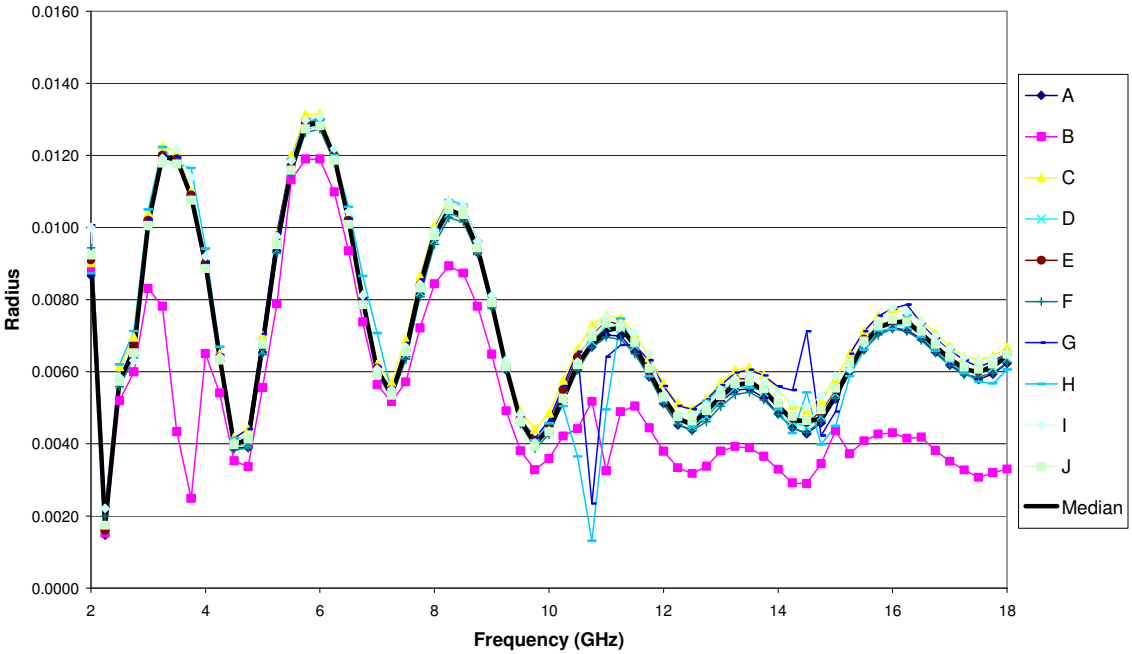

Figure 5: Circle radius for the male sliding load.

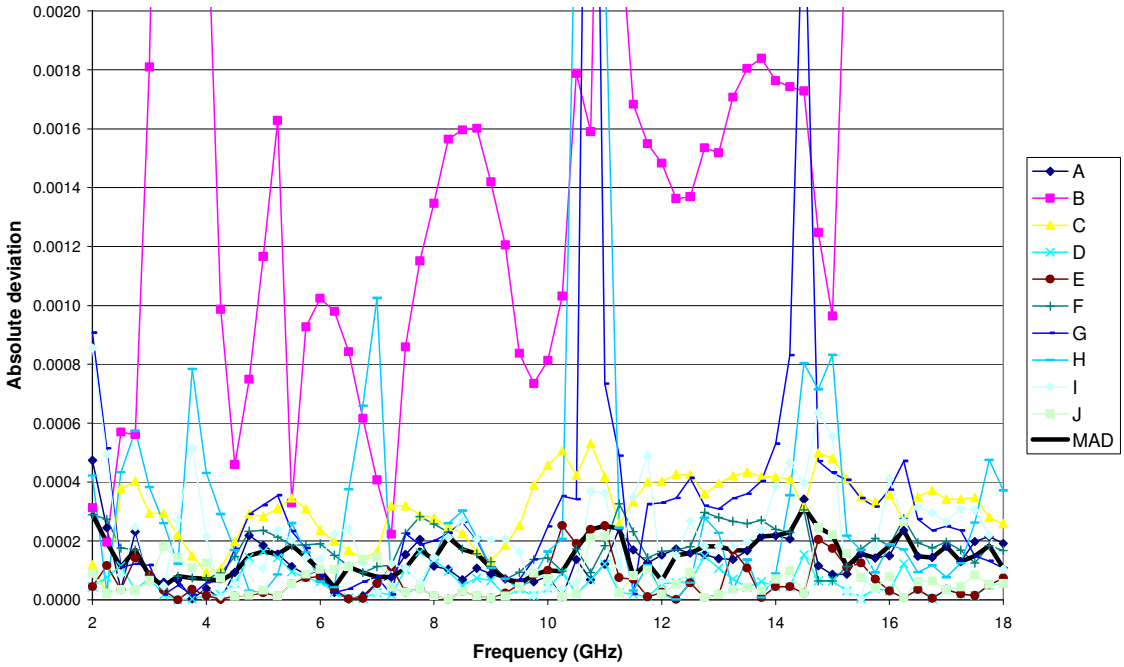

Figure 6: Absolute deviations of the measured circle radii from the median of the circle radii for the male sliding load. Also shown is the median absolute deviation (MAD).

Table 8: Percentage of measured values for each participant which are close to the consensus value for the male sliding load

Participant	Percentage of values close to consensus value	
	Circle Centre	Circle radius
A	14	78
B	75	3
C	89	6
D	46	100
E	11	95
F	68	38
G	85	28
H	31	46
I	20	38
J	91	85

Table 9: Percentage of measured values for each participant which are “unusual” for the male sliding load

Participant	Percentage of unusual values	
	Circle Centre	Circle radius
A	0	0
B	6	94
C	0	20
D	0	0
E	5	0
F	0	2
G	0	11
H	2	23
I	0	8
J	0	2

5.2 Results for the Female Sliding load before it was damaged

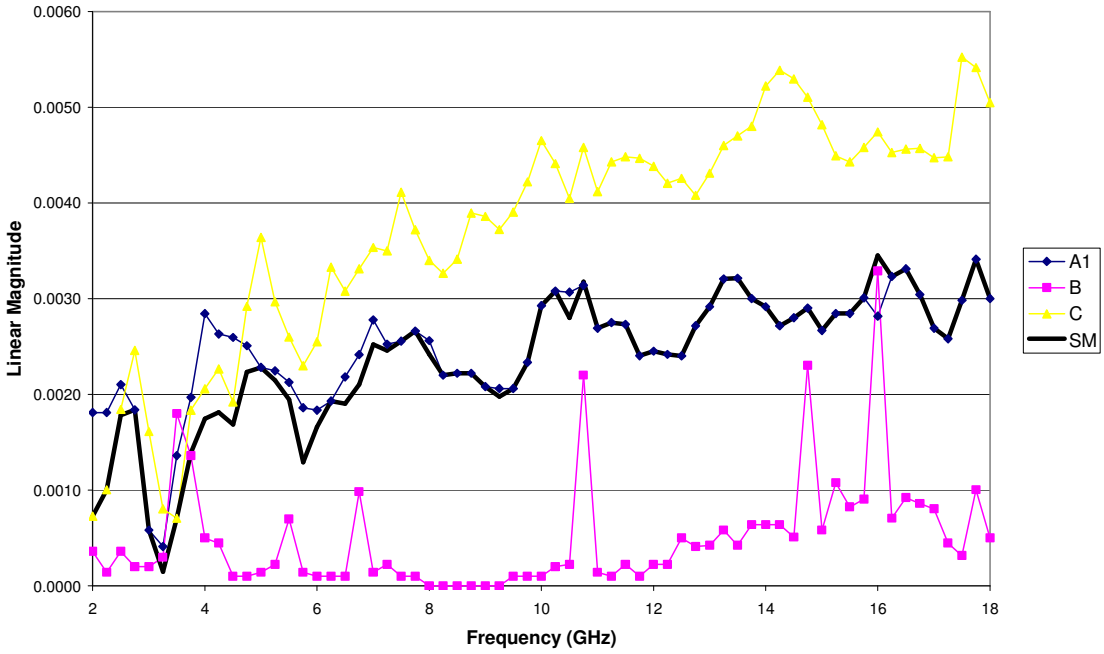

Figure 7: Linear magnitude of the circle centre for the female sliding load before it was damaged. The linear magnitude of the spatial median (SM) of the circle centres is also shown.

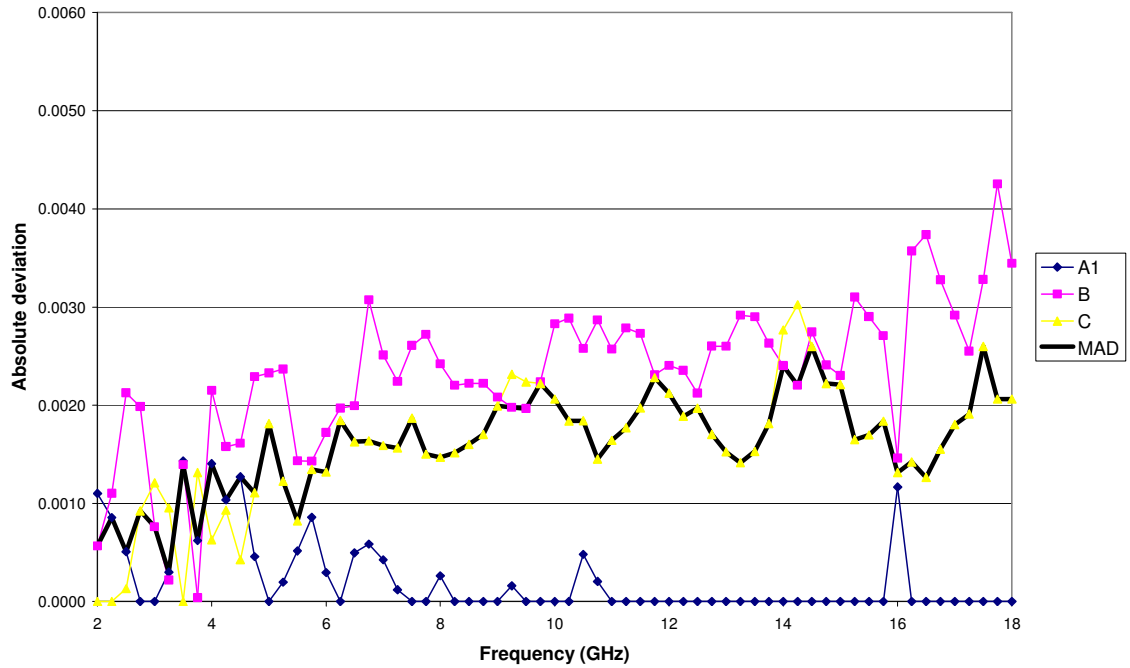

Figure 8: Absolute deviations of the measured circle centres from the spatial median of the circle centres for the female sliding load before it was damaged. Also shown is the median absolute deviation (MAD).

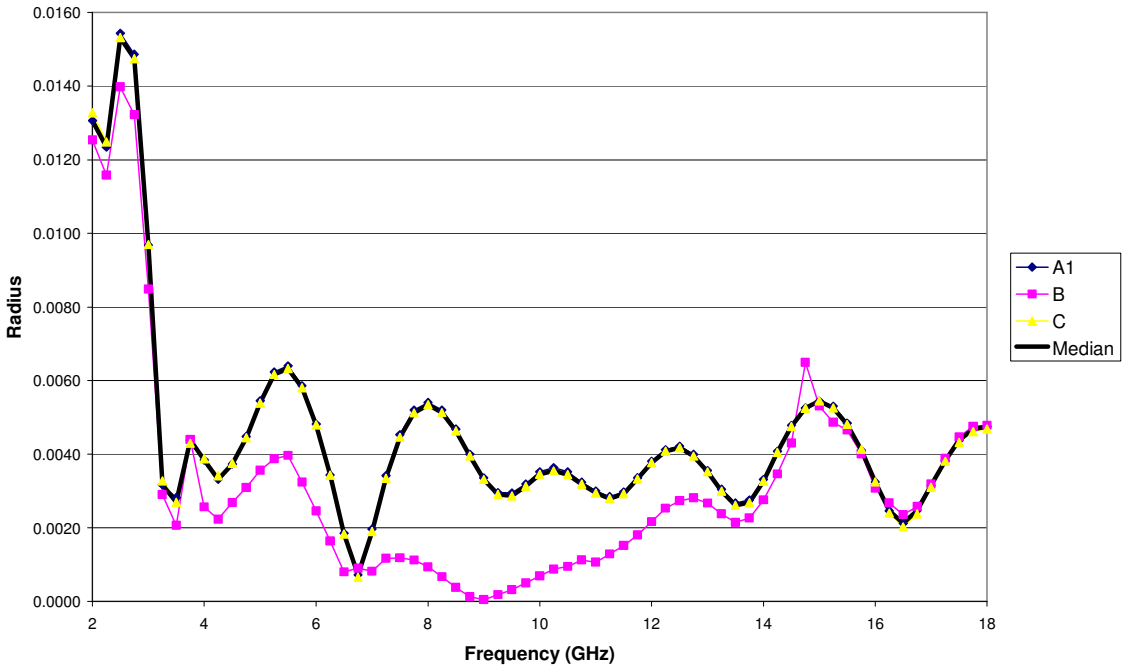

Figure 9: Circle radius for the female sliding load before it was damaged.

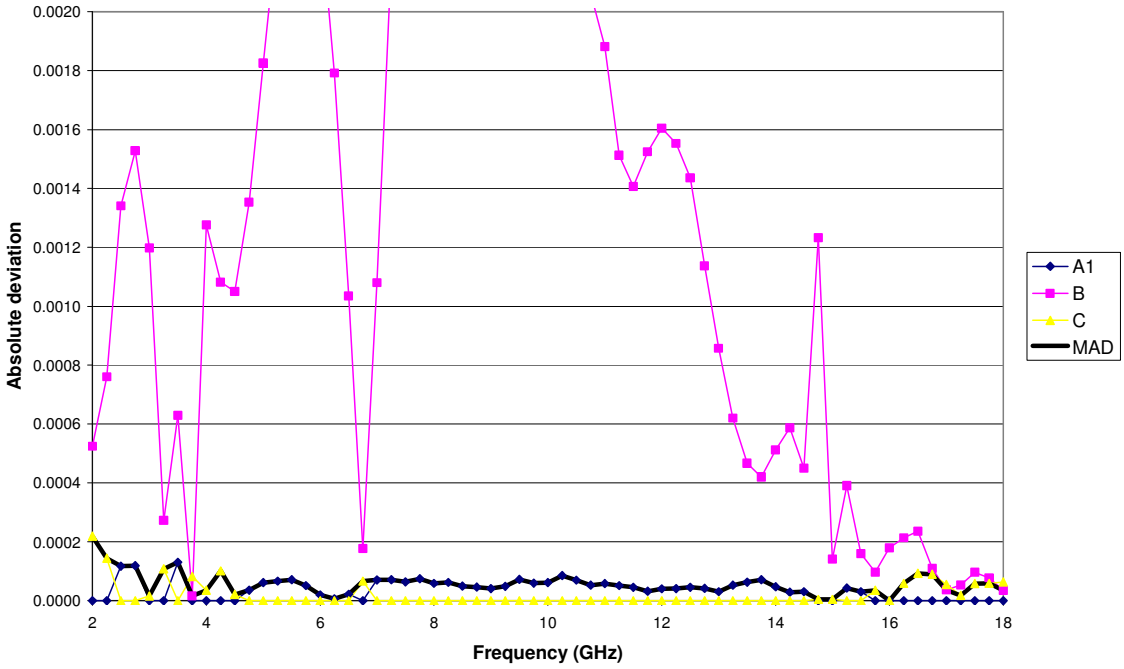

Figure 10: Absolute deviations of the measured circle radii from the median of the circle radii for the female sliding load before it was damaged. Also shown is the median absolute deviation (MAD).

Table 10: Percentage of measured values for each participant which are close to the consensus value for the female sliding load before it was damaged

Participant	Percentage of values close to consensus value	
	Circle centre	Circle radius
A1	89	100
B	8	5
C	55	95

Table 11: Percentage of measured values for each participant which are “unusual” for the female sliding load before it was damaged

Participant	Percentage of unusual values	
	Circle centre	Circle radius
A1	0	0
B	2	82
C	0	2

5.3 Results for the Female Sliding Load after it was repaired

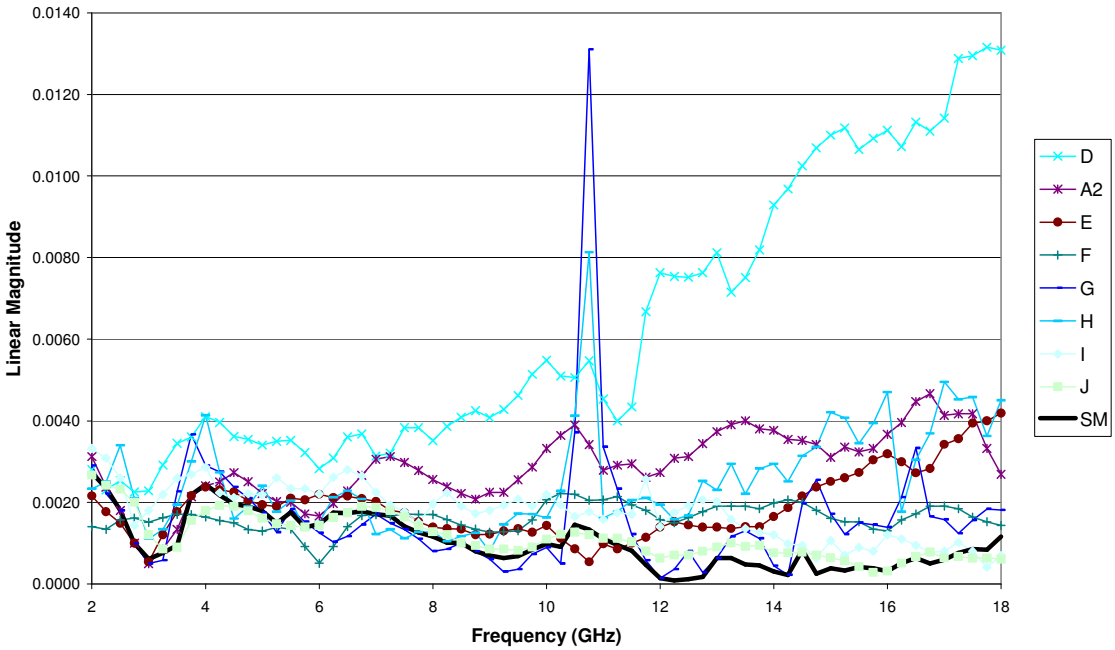

Figure 11: Linear magnitude of the circle centre for the female sliding load after it was repaired. The linear magnitude of the spatial median (SM) of the circle centres is also shown.

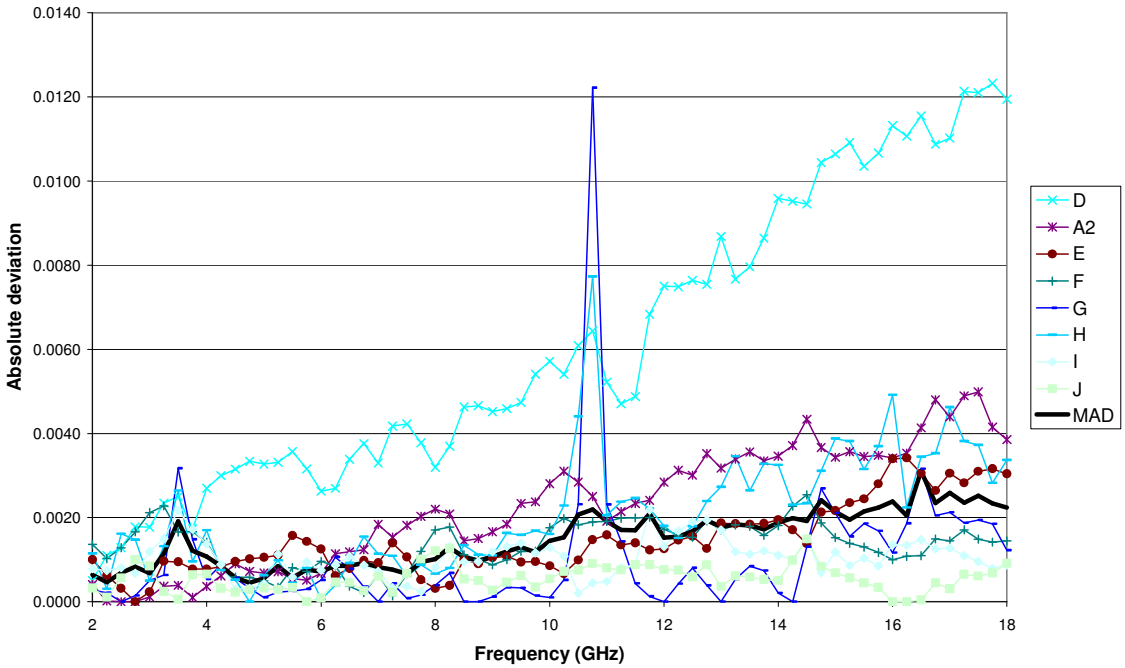

Figure 12: Absolute deviations of the measured circle centres from the spatial median of the circle centres for the female sliding load after it was repaired. Also shown is the median absolute deviation (MAD).

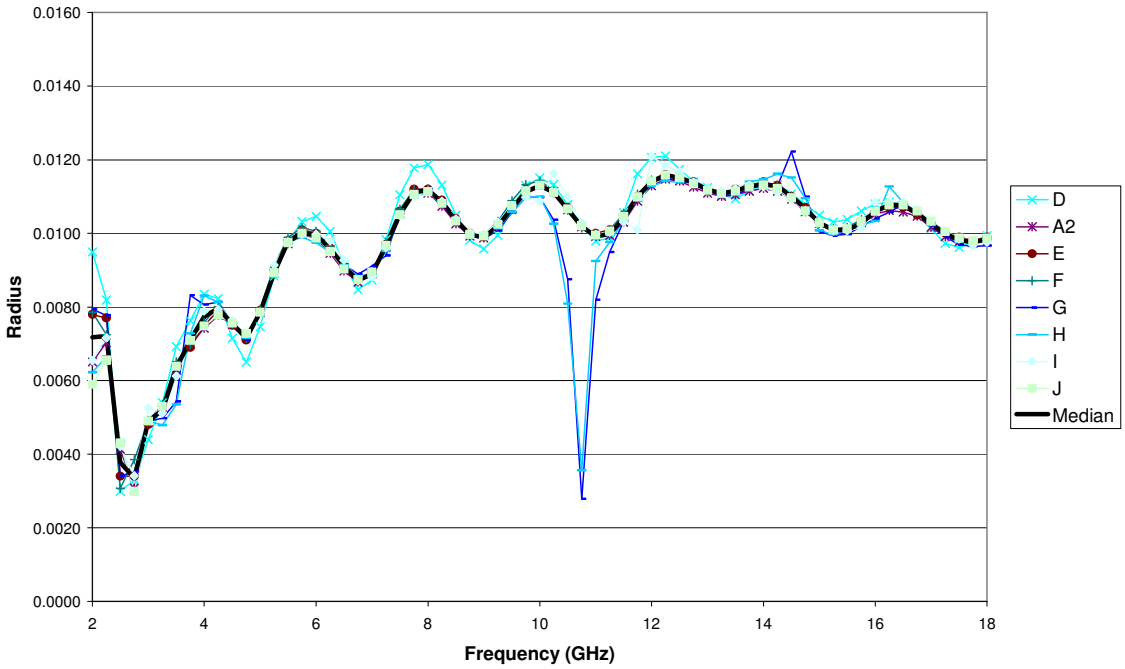

Figure 13: Circle radius for the female sliding load after it was repaired.

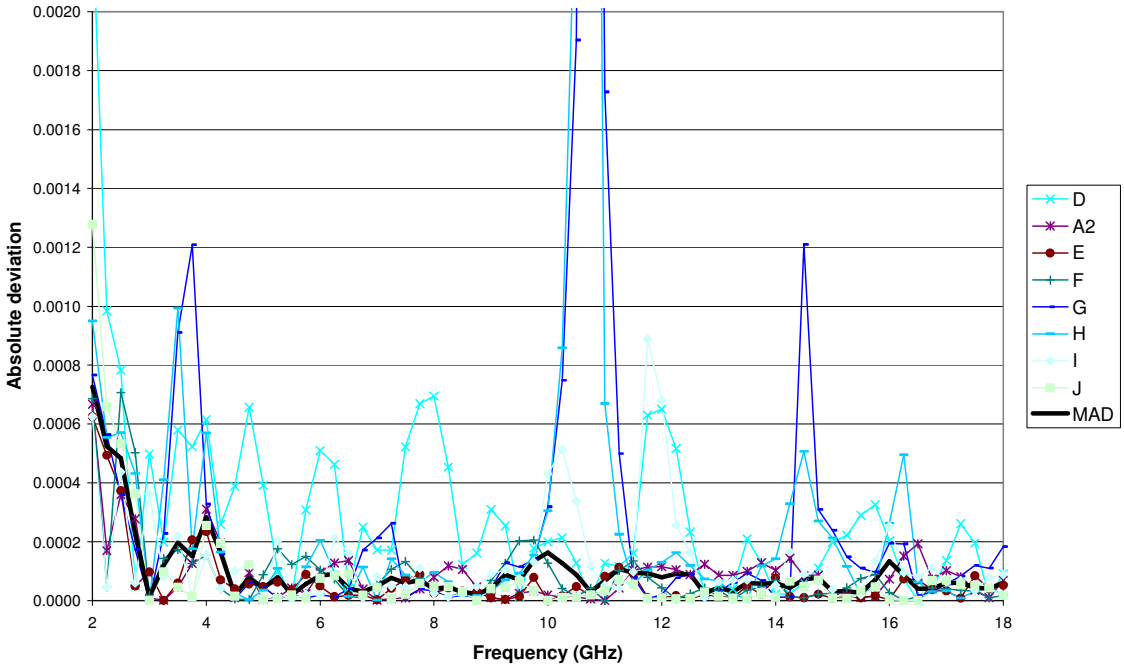

Figure 14: Absolute deviations of the measured circle radii from the median of the circle radii for the female sliding load after it was repaired. Also shown is the median absolute deviation (MAD).

Table 12: Percentage of measured values for each participant which are close to the consensus value for the female sliding load after it was repaired

Participant	Percentage of values close to consensus value	
	Circle centre	Circle radius
D	2	20
A2	22	52
E	54	78
F	58	63
G	86	46
H	22	34
I	65	45
J	92	74

Table 13: Percentage of measured values for each participant which are “unusual” for each measurand for the female sliding load after it was repaired

Participant	Percentage of unusual values	
	Circle centre	Circle radius
D	65	43
A2	0	8
E	0	2
F	0	2
G	2	25
H	0	20
I	0	14
J	0	0

5.4 Overall variability of the results

Table 14: Overall measure of variability for circle centre and circle radius (Maximum MAD for each of the measurands for each of the devices)

Device	Overall measure of variability (Maximum MAD)	
	Circle centre	Circle radius
Male sliding load	0.0022	0.0003
Female sliding load (before breakage)	0.0026	0.0002
Female sliding load (after repair)	0.0031	0.0007

6 Discussion

Generally speaking, the participants' determinations of the circle centres and circle radii are in good agreement with one another as shown by the Maximum MAD figures shown in Table 14. These figures can be converted to an equivalent standard deviation by multiplying by approximately 1.5 (assuming a normal distribution).

The participants who used only four or five slider positions in their determinations of the circle parameters (namely B, G, H and I) show unusual values at a relatively large proportion of frequencies most notably for the circle radii but also to some extent for the circle centres.

In addition, participant C obtained a relatively large number of unusual values for the circle radius for the male sliding load and participant D obtained a relatively large number of unusual values for both the circle centre and the circle radius for the female sliding load (after repair). Participant C was the only participant to use Method 2 (Mean radius method) to fit circles, all the other participants used Method 1 (Kasa's method/ Linear least squares method). This might explain the unusual values of circle radius for the male sliding load obtained by participant C that are evident in Figure 6.

6.1 Male sliding load

In the determination of the circle radius for the male sliding load, participants B, C, G and H all show a relatively large number of unusual values. Participant B deviates significantly from the consensus values at almost all frequencies. Participants C, G and H also show significant deviations from the consensus value at a smaller number of frequencies. In particular, participants G and H show a significant deviation from the consensus values for both the circle centre and the circle radius in the vicinity of 11 GHz.

6.2 Female sliding load before damage

Only three participants measured the female sliding load before it was damaged (A1, B and C). Of these, participants A1 and C agree fairly closely thereby establishing a consensus (of two!) whilst participant B differs significantly from the other two especially in the determination of the radius.

6.3 Female sliding load after repair

For the female sliding load after repair, participant D shows significant deviation from the consensus values for both the circle centre and the circle radius at a large proportion of the frequencies. Participants G, H and I also show significant deviations from the consensus value for circle radius at a smaller number of frequencies. In particular, participants G and H show a significant deviation from the consensus values for both the circle centre and the circle radius in the vicinity of 11 GHz.

7 Conclusions

A comparison of microwave measurements on sliding loads has been completed between ten leading practitioners of this type of measurement. Good agreement was obtained between the determinations of the circles defined by the sliding loads in the VRC plane. However the results indicate that four or five slider positions are probably insufficient for this type of circle determination.

8 Acknowledgements

The author would like to thank the following people for taking part in the comparison and supplying details of the measurement methods and circle fitting methods used: Steve Worrall (Deceased) and Doug Skinner (Aeroflex), Steve Harter and Pete Constable (ASAP, now Trescal), Karel Drazil (CMI), Manuel Rodriguez (INTA), Juerg Ruefenacht (METAS), Jan de Vreede (Deceased) (NMI), Masahiro Horibe (NMIJ, AIST), Martin Salter (NPL), Patrik Persson and Mikael Rydstedt (Saab Metech AB, now Bodycote Metech AB), Senel Yaran (TUBITAK-UME).

ANAMET is funded by the National Measurement Office of the UK government's Department for Business, Innovation and Skills.

9 References

[1] D M Kerns & R W Beatty, "Basic theory of waveguide junctions and introductory microwave network analysis", Pergamon Press, Oxford, 1967, Section 2.14(b), pp 89-91.

[2] G A Deschamps, "Determination of reflection coefficient and insertion loss of a waveguide junction", Appl Phys, Vol 24, No 8, pp 1046-1050, August 1953.

[3] W.C. Daywitt and G. Comas, "Measuring adapter efficiency using a sliding short circuit", IEEE Trans MTT, Vol 38, No 3, pp 231-237, March 1990.

[4] I Kasa, "Closed-form mathematical solutions to some network analyzer calibration equations", IEEE Trans IM, Vol 23, No 4, pp 8-14, December 1974.

[5] G F Engen, "Calibration technique for automated network analyzers with application to adapter evaluation", IEEE Trans MTT, Vol 22, No 12, pp 1255-1260, December 1974.

[6] A Bjorck, "Numerical methods for least squares problems", Society for Industrial and Applied Mathematics (SIAM), Philadelphia, PA, 1996.

[7] I Kasa, "A circle fitting procedure and its error analysis", IEEE Trans IM, Vol 25, No 1, pp 8-14, March 1976.

[8] J C Medley and N M Ridler, "Analysing multidimensional measurement comparison data containing occasional erratic points", *Conference on Precision Electromagnetic Measurements (CPEM) Digest*, pp 51-52, Braunschweig, Germany, 17-20 June 1996.